Tellus
SERIES B
CHEMICAL
AND PHYSICAL
METEOROLOGY
PUBLISHED BY THE INTERNATIONAL METEOROLOGICAL INSTITUTE IN STOCKHOLM

Tellus (2009), 61B, 618–624
Printed in Singapore. All rights reserved

TELLUS

Present-day contribution of anthropogenic emissions from China to the global burden and radiative forcing of aerosol and ozone

By C. R. HOYLE[1,3]*, G. MYHRE[2] and I. S. A. ISAKSEN[1,2], [1]*Department of Geosciences, University of Oslo, Norway;* [2]*Center for International Climate and Environmental Research—Oslo (CICERO), Norway;* [3]*Institute for Atmospheric and Climate Science, ETH Zurich, Switzerland*

(Manuscript received 21 July 2008; in final form 20 March 2009)

ABSTRACT

The effect of anthropogenic emissions from China on global burdens of ozone, sulphate, organic carbon (OC) and black carbon (BC) aerosols is examined, using the three-dimensional chemistry transport model Oslo CTM2. Two model simulations were performed, the first with global present-day emissions and the second with the anthropogenic emissions from China set to their pre-industrial levels. The global radiative forcing for these species is then calculated. Industrial emissions from China are found to account for a 4–5% increase in the global burden of OC aerosol, the change in secondary organic aerosol being slightly less than that of primary organic aerosol. A 10% increase in the global sulphate aerosol burden is calculated, and the increase in BC is 23%. The global radiative forcing of aerosols from China was calculated to be −62, −3.7, −13 and 89 mW m^{-2}, for sulphate, secondary organic, primary organic and BC aerosols, respectively. The increase in ozone causes a forcing of 77 mW m^{-2}.

1. Introduction

The rapid industrial development of China has lead to large increases in industrial emissions. As well as increasing burdens of primary aerosol species, such as black and organic carbon (OC), the industrial emissions influence the chemistry of the atmosphere.

Several studies have looked at the increase in aerosol species over China and have calculated the regional radiative forcing effects. Estimates of the radiative forcing over China from sulphate and black carbon (BC) aerosols, have been calculated by Giorgi et al. (2002), who found top of the atmosphere forcings of −1 to −15 and 0.5 to 2 W m^{-2} for anthropogenic sulphate and fossil fuel BC, respectively, depending on season and location. The forcing due to sulphate, OC, BC, mineral dust, sea salt and methane sulphonic acid (MSA) particles was calculated by Qian et al. (2003), with total values ranging from −1 to −9 W m^{-2}, depending on season and location.

More global effects of increases in Asian aerosols were investigated by Menon et al. (2002), using a global climate model with enhanced aerosol over China and India. Increases in BC were found to influence not just regional climate, but also the large-scale circulation.

In addition to increases in aerosol burdens, industrial emissions can affect tropospheric ozone concentrations. Previous studies have looked at the influence of ozone exported from Asia on air quality in the United States (Berntsen et al., 1999; Jacob et al., 1999, 2003) or in Europe (Li et al., 2002). Sudo and Akimoto (2007) found ozone from the boundary layer and free troposphere over Asia to have significant impacts on the ozone concentrations in the middle to upper troposphere almost globally. Additionally, Unger et al. (2008) examined the importance of regional differences in precursor emissions from particular industry sectors for the production of O_3 and other secondary pollutants.

It is important to separate the contribution of emissions from different countries or regions to the global burden of short lived compounds that have an influence on the Earth's climate. A study by Reddy and Boucher (2007) found global warming potentials (GWP) of between 374 and 677 for BC emitted in different regions. Further, it was shown by Berntsen et al. (2006) that due to regional differences in deposition rates and solar insolation, a given quantity of a shortlived compound can have a very different forcing on the climate, depending on where it is emitted. Berntsen et al. (2006) found that an equal reduction of emissions of OC would lead to a reduction in the global OC burden

*Corresponding author.
e-mail: c.r.hoyle@geo.uio.no,
Address: Swiss Federal Institute of Technology (ETH), Institute for Atmospheric and Climate Science, Universitatstrasse 16, CH-8092 Zurich, Switzerland
DOI: 10.1111/j.1600-0889.2009.00424.x

by 6.6 μg(C)m^{-2} if the reduction was made in South Asia, but only by 3.3 μg(C)m^{-2} if the reduction was made in China. Similarly, an emission reduction in China was found to have the lowest change in global average annual radiative forcing from the regions studied.

In this study, the total contribution of industrial emissions from China to OC and BC aerosol, sulphate aerosol and tropospheric ozone is calculated. Both primary (directly emitted) and secondary (formed in situ) organic aerosol species (POA and SOA, respectively) are modelled, and the global mean radiative forcings of the aerosol species and ozone are calculated. The formation of SOA via the gas phase oxidation of biogenic and anthropogenic hydrocarbons is explicitly calculated, so that changes in the oxidant fields and available mass for partitioning will affect the amount of SOA formed. In addition, we separate the radiative forcing contributions of POA from fossil or biofuel combustion and from biomass burning.

In the next section, the models used, as well as the simulations that were performed are described. In Section 3, the results are presented and discussed, and in Section 4, a summary and conclusions are provided.

2. Modelling tools

2.1. The Oslo CTM2

The Oslo CTM2 is a three dimensional off-line chemistry transport model, which was run in T42 (approximately 2.8° × 2.8°) resolution for this study. The meteorological data used was generated by running the Integrated Forecast System (IFS) of the European Centre for Medium Range Weather Forecasts (ECMWF) for the year 2004, and was updated (offline) in the CTM every 3 hr. The same meteorological data were used for both simulations.

The model is divided into 40 layers between the surface and 10 hPa. The chemical time step in the troposphere was 15 min, and the transport time step is based on the Courant–Friedrichs–Lewy (CFL) criteria. In the free troposphere, the greatest possible transport time step was 1 hr, and in the boundary layer it was 15 min.

The aerosol species included in the model for this study were SOA, POA, sulphate and BC. The implementation and validation of these aerosol species in the Oslo CTM2 are described in Hoyle et al. (2007), Myhre et al. (2003a), Berntsen et al. (2006) and Berglen et al. (2004). POA is assumed to be emitted directly to the atmosphere and SOA in the Oslo CTM2 is formed via the equilibrium partitioning of semi volatile species, formed as the result of the gas phase oxidation of eight classes of precursor species. In this study, SOA is assumed only to condense on existing organic aerosol.

The global aerosol model has been extensively validated against in situ measurements and remote sensing data from the ground and from space (Myhre et al., 2008b). It has also been compared with aircraft data and other aerosol observations during campaigns (Myhre et al., 2003a, 2008a,b,c).

2.2. Model experiments and emissions

Two model runs were performed, the first (R_{present}) is representative of the present-day atmosphere, whereas for the second (R_{noChina}), anthropogenic emissions in China were reduced to pre-industrial levels. In all other respects, the two runs were identical. A comparison of these two simulations provides the burdens of aerosol and ozone in the present-day atmosphere, which result from emissions from China. Table 1 summarizes the global emissions of relevant species in the two model runs.

Several recent studies have indicated that the industrial emissions from China are increasing very rapidly (Richter et al., 2005; van der A et al., 2008; Stavrakou et al., 2008). One of the general problems of global chemistry modelling in such a situation is that global, gridded emission inventories for different species, often being the work of different research groups, are not created at the same time and are not representative of exactly the same time periods. Further, due to the time taken to collect and compile the emissions data, there is a substantial lag between an emission year and the availability of an

Table 1. The emissions used in the two model runs, including and not including anthropogenic emissions from China

Species	R_{present}	R_{noChina}	Diff.	2000	Source
OC (Tg(C) yr^{-1})	30.4	28.2	2.2	2.6	Bond et al. (2004), van der Werf (2006)
BC(Tg(C) yr^{-1})	7.4	6.0	1.4	1.1	Bond et al. (2004), van der Werf (2006)
SO_2(Tg(SO_2) yr^{-1})	134	107	27	27.6	Dentener et al. (2006)
CO (Tg(CO)yr^{-1})	1061	947	114	137	Granier et al. (2005)
NO_x(Tg(N)yr^{-1})	46.7	41.9	4.8	5.1	Granier et al. (2005)
Biogenic VOC (Tg(C)yr^{-1})	386	386	0	-	Guenther et al. (1995)
Anthropogenic VOC (Tg yr^{-1})	21.6	12.8	8.8	-	M. G. Schultz et al. (unpublished data)
Isoprene (Tg yr^{-1})	220	220	0	-	Granier et al. (2005), IPCC (2001)

Noet: The emission difference between the two scenarios is given in the column labelled 'Diff.', whereas the emission values for 2000(Ohara et al., 2007) are given in the column marked'2000'. Biogenic VOC includes terpenes and other biogenic volatile organic compounds, except isoprene, which is listed separately.

inventory describing it. The emissions listed in Table 1 come from a variety of inventories, representative of several different years. However, a comparison with a recent assessment of total emissions from different countries (Ohara et al., 2007) shows that the anthropogenic emissions from China used here are consistent with levels for the year 2000, especially when the range of emissions from other inventories, compared in table 6 of Ohara et al. (2007) is taken into account. More recent biomass burning OC and BC data was available, therefore emissions for the year 2004 were used.

2.3. *Radiative transfer model*

The radiative forcing was calculated using a radiative transfer model. A short-wave multistream model, using the discrete-ordinate method of Stamnes et al. (1988) was adopted for the aerosol calculations. The radiative transfer model includes the radiative effects of aerosols, clouds, Rayleigh scattering, and absorption by gases. The optical properties of BC aerosol are calculated under the assumption of internal mixing of the hygroscopic BC particles. To take into account internal mixture of BC as coated sphere, increasing the absorption for hydrophilic BC particles by 50% (but with no change for the hydrophobic BC particles) has been suggested as a simplified method (Bond et al., 2006).

The calculations were performed at the same resolution and with the same meteorological data as the model runs. A more detailed description of the radiative transfer model can be found in Myhre et al. (2002). Aerosol optical properties are described in Myhre et al. (2007). The radiative transfer model used for the ozone calculations is described in Myhre et al. (2000) and Gauss et al. (2006).

3. Results and discussion

The anthropogenic emissions from China are found to have a substantial effect over the Pacific Ocean, as well as close to the source, over China. The annual mean fraction increase in O_3, both at the surface and for the total column, is shown in Fig. 1. Near the main source region in China, the O_3 at the surface is almost doubled, whereas over larger regions, the increase is between 10% and 20%. Small effects are seen to the west of China, whereas to the east, O_3 increases of 10%–20% reach as far as the west coast of North America. The emissions from China are found to cause increases in surface O_3 greater than 4%, almost everywhere in the Northern Hemisphere. Regions where the effect of China related O_3 is low tend to be where anthropogenic emissions are high, making the extra O_3 from Chinese emissions less significant.

For the total O_3 column, the increases are up to 20% near the source regions, elsewhere between 2% and 6%, with the main increases being limited to the tropics and a small effect extending to high northern latitudes. The limitation of the larger increases in ozone to the northern tropics and extra tropics is due to the relatively short photochemical lifetime of tropospheric ozone. The predominant westerlies transport the ozone eastward of China, and slower transport processes carry it to the north and south of the formation area. The increases in ozone in the low latitude Southern Hemisphere can be explained by the extension of the southern transport effect of the Northern Hemisphere Hadley cell into the Southern Hemisphere during winter. CO, being longer lived than ozone, may be transported into the Southern Hemisphere, enhancing ozone formation there, after oxidation.

The absolute change in SOA (Figs. 2a and c) and POA (Figs. 2b and d) at the surface and in the whole column is shown in Fig. 2. The changes in SOA near the surface are restricted to the east coast of China, with maximum values of 1–2 μgm^{-3}. The minor decreases in SOA abundance over ocean areas are due to the general reduction in global OH concentrations that emissions of CO and hydrocarbons from China caused. In the column values, the increase in SOA related to industrial emissions from China extends east from the coast, over Japan. The changes in POA are larger than in SOA, with values of up to

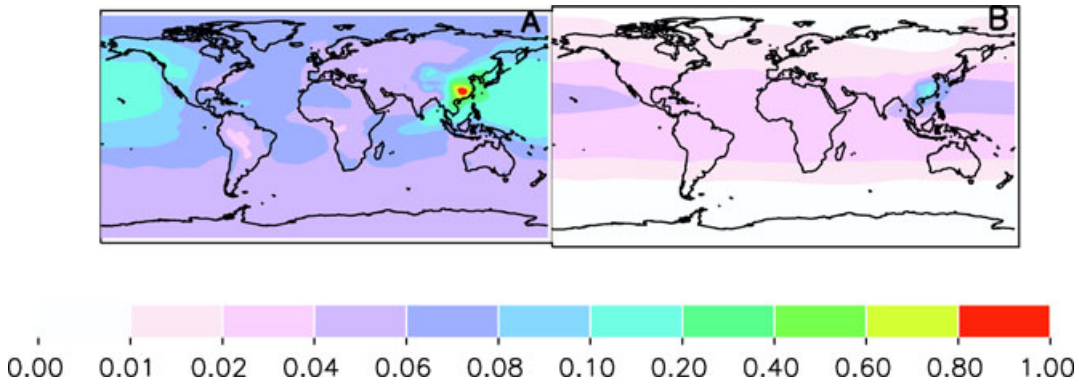

Fig. 1. The change in ozone due to present-day emissions from China, as a fraction of ozone values when emissions from China are set to pre-industrial levels. Panel a shows the change at the surface, panel b shows the change in the total column.

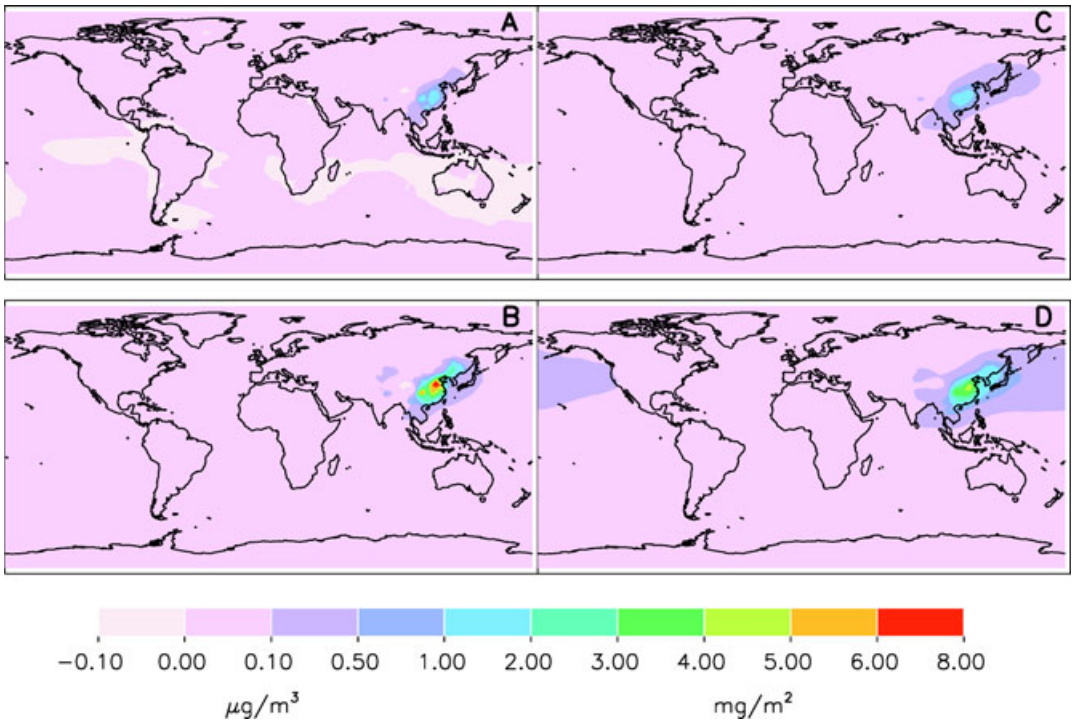

Fig. 2. The absolute change in SOA at the surface and in the column (panels a and c), when industrial emissions from China are not included. Panels b and d show the same, for POA.

6–8 μg m^{-3} at the surface, and an increase of 0.1–0.5 μg m^{-2} extending to the North American west coast.

The fractional change in aerosol caused by anthropogenic emissions from China is shown in Fig. 3. Figs. 3a–d show the annual mean surface changes, while Figs. 3e–h show the annual mean change in the total column of each type of aerosol. For SOA (Figs. 3a and e), increases of up to 10 times are seen near source regions. To the east, increases of up to 60% are seen over the Pacific; however, near the coast of North America, the effect decreases, as local emissions begin to dominate. Although these are large fractional increases, as can be seen in Fig. 2, the actual change in mass of SOA over the Pacific is rather low. In the column, the pattern is similar, with a lower fraction increase.

The changes in the POA (Figs. 3b and f) distribution are similar to those of SOA; however, the effect is larger. Near the source, there is a 40–90-fold increase in the POA burden at the surface, although concentrations are still more than doubled in the middle of the Pacific. Again, the significance of the Chinese emissions decreases rapidly near the North American coast, and the actual concentration over the Pacific is low. An interesting feature in the POA plots, particularly in the total column, is the transport of aerosol into the Arctic.

Increases in sulphate aerosol of more than a factor of 10 are seen near the most industrialized areas in China, particularly along the east coast. Increases of up to 20% are transported as far as North America. In the tropics, there are small decreases in sulphate due to lower OH concentrations and therefore reduced oxidation of SO_2. The reduction in global OH concentrations was also predicted by Rae et al. (2007) to lead to less sulphate aerosol.

The biggest differences between the two model runs are seen in BC aerosol. In Figs. 3d and h, the increases in BC reach across the Pacific, and in the column values, even over North America. The growth in BC concentrations at the surface since pre-industrial times in China is very large. BC emitted in China is also seen, mostly in the column values, to be transported to high northern latitudes and the Arctic.

The annual mean burden of the modelled aerosol species for both model runs is listed in Table 2. Reducing the emissions from China to pre-industrial levels has a significant impact on the annual mean global aerosol burden, particularly in the case of sulphate and BC, giving reductions of 5.0%, 4.0%, 10% and 23% for POA, SOA, sulphate and BC, respectively. The main contribution to the change in POA is from fossil fuel rather than biomass burning. The change in SOA burden is mostly due to the higher POA concentrations in R_{present}, providing more mass for partitioning of SOA; however, the contribution of anthropogenic SOA precursors to condensed SOA is also slightly larger in R_{present} than R_{noChina} (9.1% and 8.3% of the total burden, respectively).

From the changes in aerosol and ozone concentrations, radiative forcings have been calculated (Table 3). The largest is a positive forcing of 89 mW m^{-2}, caused by the increase in BC. The forcing from tropospheric O_3 is 77 mW m^{-2}. A large

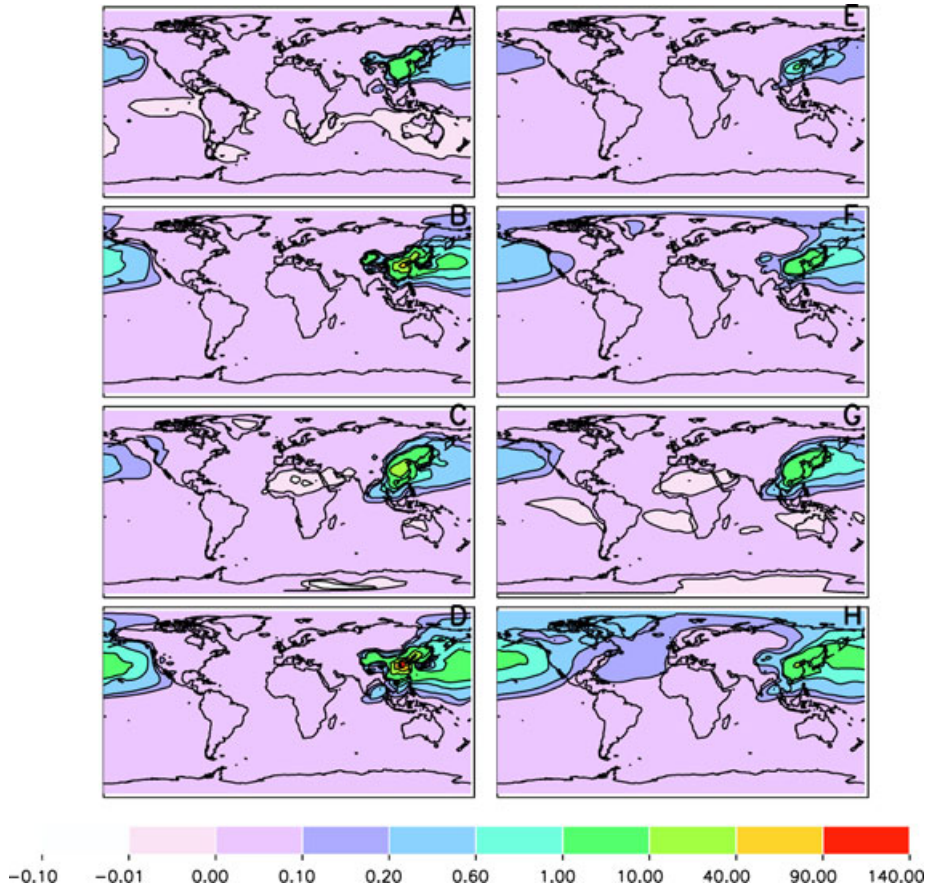

Fig. 3. The increase in the modelled aerosol species due to emissions from China, as a fraction of the pre-industrial values. Panels on the left-hand side are for the surface, while panels on the right-hand side show the change in the total column. Panels a and e: SOA; panels b and f: POA; panels c and g: Sulphate and panels d and h: BC.

Table 2. The annual mean global burdens of the different aerosol species and the percentage increase due to Chinese emission

Species	R_{present}	R_{noChina}	Percentage change
POA	0.6	0.57	5
SOA	0.50	0.48	4
Sulphate	1.80	1.64	10
BC	0.16	0.13	23

Note: In run R_{noChina}, 54% of the BC burden is from fossil fuel and biofuel combustion (60% for run R_{present}).The remainder is from biomass burning.

Table 3. The radiative forcing of aerosol species and ozone resulting from Chinese emissions

Species	Radiative forcing (mW m^{-2})
POA_F	−13.0
POA_{Bio}	−0.2
SOA	−3.7
O_3	77.3
Sulphate	−62.3
BC	89.0

Note: POA_F is primary organic aerosol from fossil and biofuel burning, whereas POA_{Bio} is from biomass burning.

negative forcing is caused by sulphate aerosol. The increased SOA concentrations contribute nearly −4 mW m^{-2}, whereas the contribution from the fraction of POA from biomass burning is very minor. The radiative forcing of POA from fossil and biofuel emissions in China is around 10% of the mean global value calculated from the models in Schulz et al. (2006). Similarly, the radiative forcing of the O_3 change accounts for around 25% of the forcing from global O_3 change since the pre-industrial times (IPCC, 2007). Including internal mixing for BC increases the importance of BC, but even if internal mixing is ignored, the

contribution of BC from China is a significant fraction of the global BC abundance.

4. Summary and conclusions

The change in abundance of O_3, as well as SOA, POA, BC and sulphate aerosols due to emissions from China has been calculated. Near the emission sources, the aerosol burdens are far greater when the present-day emissions from China are included; however, elevated aerosol burdens for SOA and POA extend east of China, especially in the total column. Over the ocean, although the fractional change in concentration is large, the total mass of aerosol is very low. BC from China causes a 20%–40% increase in the total column mass of BC over North America; however, the long-range transport of the other aerosol species is much smaller than the burden over North America due to the local emissions. The model predicts that emissions of POA from China slightly increase the total column of POA above the Arctic. Emissions from China are found to cause significant increases in sulphate aerosol; however, small decreases are observed in the tropical column values, due to the globally lower OH concentrations in the run with emissions from China. In terms of radiative forcing, the anthropogeic emissions from China lead to an increase in tropospheric ozone, resulting in a positive forcing of 77 mW m^{-2} or around a quarter of the total global radiative forcing from tropospheric ozone. The positive forcing from BC (89 mW m^{-2}) is even larger than that of ozone, similar in magnitude to the negative forcing from sulphate aerosol, whereas the negative forcing from OC aerosol is much smaller. The radiative forcing of POA from fossil and bio fuel combustion in China accounts for a significant fraction of the total global value. The net radiative forcing of the Chinese emissions of the species considered here is approximately 87 mW m^{-2}, and that due only to the aerosol species is approximately 10 mW m^{-2}.

5. Acknowledgments

This work was carried out with funding from the EU projects Biosphere–Aerosol–Cloud–Climate Interactions (BACCI) and EUCAARI (European Integrated Project on Aerosol Cloud Climate and Air Quality Interactions), as well as from the Norwegian Research Council.

References

van der A, R. J., Eskes, H. J., Boersma, K. F., van Noije, T. P. C., Van Roozendael, M. and co-authors. 2008. Trends, seasonal variability and dominant NO_x source derived from a ten year record of NO_2 measured from space. *J. Geophys. Res.—Atmospheres* **113**, D4. doi:10.1029/2007JD009021.

Berglen, T. F., Berntsen, T. K., Isaksen, I. S. A. and Sundet, J. K. 2004. A global model of the coupled sulfur/oxidant chemistry in the troposphere: the sulfur cycle. *J. Geophys. Res.* **109**, D19310, doi:10.1029/2003JD003948.

Berntsen, T., Karlsdottir, S. and Jaffe, D. 1999. Influence of Asian emissions on the composition of air reaching the North Western United States. *Geophys. Res. Lett.* **26**, 2171–2174.

Berntsen, T., Fuglestvedt, J., Myhre, G., Stordal, F. and Berglen, T. 2006. Abatement of greenhouse gases: does location matter? *Clim. Change* **74**, 377–411, doi:10.1007/s10584-006-0433-4.

Bond, T. C., Streets, D. G., Yarber, K. F., Nelson, S. M., Woo, J.-H. and co-authors. 2004. A technology-based global inventory of black and organic carbon emissions from combustion. *J. Geophys. Res.—Atmosphere* **109**, doi:10.1029/2003JD003697.

Bond, T. C., Habib, G. and Bergstrom, R. W. 2006. Limitations in the enhancement of visible light absorption due to mixing state. *J. Geophys. Res.—Atmospheres* **111**, D20, doi:10.1029/2006JD007315.

Dentener, F., Kinne, S., Bond, T., Boucher, O., Cofala, J. and co-authors. 2006. Emissions of primary aerosol and precursor gases in the years 2000 and 1750 prescribed data-sets for AeroCom. *Atmos. Chem. Phys.* **6**, 4321–4344.

Gauss, M., Myhre, G., Isaksen, I. S. A., Grewe, V., Pitari, G. and co-authors. 2006. Radiative forcing since preindustrial times due to ozone change in the troposphere and the lower stratosphere. *Atmos. Chem. Phys.* **6**, 575–599.

Giorgi, F., Bi, X. and Qian, Y. 2002. Direct radiative forcing and regional climatic effects of anthropogenic aerosols over East Asia: a regional coupled climate-chemistry/aerosol model study. *J. Geophys. Res.—Atmosphere* **107**, D20, doi:10.1029/2001JD001066.

Granier, C., Lamarque, J. F., Mieville, A., Muller, J. F., Olivier, J. and co-authors. 2005. Poet, a database of surface emissions of ozone precursors. Available at: http://www.aero.jussieu.fr/projet/ACCENT/POET.php

Guenther, A., Hewitt, C. N., Erickson, D., Fall, R., Geron, C. and co-authors. 1995. A global model of natural volatile organic compound emissions. *J. Geophys. Res.* **100**(D5), 8873–8892, doi:10.1029/94JD02950.

Hoyle, C. R., Berntsen, T., Myhre, G. and Isaksen, I. S. A. 2007. Secondary organic aerosol in the global aerosol - chemical transport model Oslo CTM2. *Atmos. Chem. Phys.* **7**, 5675–5694.

IPCC 2001. *Climate Change 2001: The Scientific Basis. Contribution of Working Group I to the Third Assessment Report of the Intergovernmental Panel on Climate Change.* Cambridge University Press, Cambridge, United Kingdom and New York, NY, USA, 881pp.

IPCC 2007. *Climate Change 2007: Synthesis Report. Contribution of Working groups I, II and III to the Fourth Assessment Report of the Intergovernmental Panel on Climate Change.* IPCC, Geneva, Switzerland, 104pp.

Jacob, D., Logan, J. and Murti, P. 1999. Effect of rising Asian emissions on surface ozone in the United States. *Geophys. Res. Lett.* **26**, 2175–2178.

Jacob, D., Crawford, J., Kleb, M., Connors, V., Bendura, R. and co-authors. 2003. Transport and Chemical Evolution over the Pacific (TRACE-P) aircraft mission: design, execution, and first results. *J. Geophys. Res.—Atmosphere* **108**(D20), 1–19. doi:10.1029/2002JD003276.

Li, Q., Jacob, D., Bey, I., Palmer, P., Duncan, B. and co-authors. 2002. Transatlantic transport of pollution and its effects on surface ozone in Europe and North America. *J. Geophys. Res.–Atmosphere* **107**(D13). doi:10.1029/2001JD001422.

Menon, S., Hansen, J., Nazarenko, L. and Luo, Y. 2002. Climate effects of black carbon aerosols in China and India. *Science* **297**, 2250–2253.

Myhre, G., Karlsdottir, S., Isaksen, I. and Stordal, F. 2000. Radiative forcing due to changes in tropospheric ozone in the period 1980 to 1996. *J. Geophys. Res.—Atmosphere* **105**(D23), 28 935–28 942.

Myhre, G., Jonson, J. E., Bartnicki, J., Stordal, F. and Shine, K. P. 2002. Role of spatial and temporal variations in the computation of radiative forcing due to sulphate aerosols: a regional study. *Q. J. R. Meteorol. Soc.* **128**, 973–989.

Myhre, G., Berntsen, T. K., Haywood, J. M., Sundet, J. K., Holben, B. N. and co-authors. 2003a. Modelling the solar radiative impact of aerosols from biomass burning during the Southern African Regional Science Initiative (SAFARI-2000) experiment. *J. Geophys. Res.—Atmosphere* **108**(D13), 8501. doi:10.1029/2002JD002313.

Myhre, G., Grini, A., Haywood, J. M., Stordal, F., Chatenet, B. and co-authors. 2003b. Modeling the radiative impact of mineral dust during the Saharan Dust Experiment (SHADE) campaign. *J. Geophys. Res.* **108**, D18, doi:10.1029/2002jd002566.

Myhre, G., Bellouin, N., Berglen, T. F., Berntsen, T. K., Boucher, O. and co-authors. 2007. Comparison of the radiative properties and direct radiative effect of aerosols from a global aerosol model and remote sensing data over ocean. *Tellus* **59B**, 115–129. doi:10.1111/j.1600-0889.2006.00226.x.

Myhre, G., Berglen, T. F., Hoyle, C. R., Christopher, S. A., Coe, H. and co-authors. 2008a. Modelling of chemical and physical aerosol properties during the ADRIEX aerosol campaign. *Q. J. R. Meteorol. Soc.* **135**, doi:10.1002/qj.350.

Myhre, G., Berglen, T. F., Johnsrud, M., Hoyle, C. R., Berntsen, T. K. and co-authors. 2008b. Radiative forcing of the direct aerosol effect using a multi-observation approach. *Atmos. Chem. Phys. Discuss.* **8**, 12 823–12 886.

Myhre, G., Hoyle, C. R., Berglen, T. F., Johnson, B. T. and Haywood, J. M. 2008c. Aerosol modelling of the solar radiative impact of aerosols from biomass burning during the DABEX campaign. *J. Geophys. Res.* **113**, D00C16, doi:10.1029/2008JD009857.

Ohara, T., Akimoto, H., Kurokawa, J., Horii, N., Yamaji, K. and co-authors.Hayasaka, T. 2007. An Asian emission inventory of anthropogenic emission sources for the period 1980–2020. *Atmos. Chem. Phys.* **7**, 4419–4444.

Qian, Y., Leung, L., Ghan, S. and Giorgi, F. 2003. Regional climate effects of aerosols over China: modeling and observation. *Tellus* **55B**, 914–934.

Rae, J. G. L., Johnson, C. E., Bellouin, N., Boucher, O., Haywood, J. M. and co-authors. 2007. Sensitivity of global sulphate aerosol production to changes in oxidant concentrations and climate. *J. Geophys. Res.—Atmosphere* **112**, D10, doi:10.1029/2006JD007826.

Reddy, M. S. and Boucher, O. 2007. Climate impact of black carbon emitted from energy consumption in the world's regions. *Geophys. Res. Lett.* **34**, doi:10.1029/2006GL028904.

Richter, A., Burrows, J., Nuss, H., Granier, C. and Niemeier, U. 2005. Increase in tropospheric nitrogen dioxide over China observed from space. *Nature* **437**, 129–132, doi:10.1038/nature04092.

Schulz, M., Textor, C., Kinne, S., Balkanski, Y., Bauer, S. and co-authors. 2006. Radiative forcing by aerosols as derived from the AeroCom present-day and pre-industrial simulations. *Atmos. Chem. Phys.* **6**, 5225–5246.

Stamnes, K., Tsay, S.-C., Jayaweera, K. and Wiscombe, W. 1988. Numerically stable algorithm for discrete-ordinate-method radiative transfer in multiple scattering and emitting layered media. *Appl. Opt.* **27**, 2502–2509.

Stavrakou, T., Muller, J.-F., Boersma, K. F., De Smedt, I. and van der A, R. J. 2008. Assessing the distribution and growth rates of NO_x emission sources by inverting a 10-year record of NO_2 satellite columns. *Geophys. Res. Lett.* **35**. doi:10.1029/2008GL033521.

Sudo, K. and Akimoto, H. 2007. Global source attribution of tropospheric ozone: long-range transport from various source regions. *J. Geophys. Res.–Atmosphere* **112**, D12, doi:10.1029/2006JD007992.

Unger, N., Shindell, D. T., Koch, D. M. and Streets, D. G. 2008. Air pollution radiative forcing from specific emissions sectors at 2030. *J. Geophys. Res.—Atmosphere* **113**, D2, doi:10.1029/2007JD008683.

van der Werf, G. R., Randerson, J. T., Giglio, L., Collatz, G. J., Kasibhatla, P. S. and co-authors, 2006. Interannual variability in global biomass burning emissions from 1997 to 2004. *Atmos. Chem. Phys.* **6**, 3423–3441.